Control System Design for a STATCOM using Complex Transfer Function

N. VORAPHONPIPUT[a], I. NGAMROO[b], S. CHATRATANA[c]
[a]Electricity Generating Authority of Thailand, 11130 THAILAND
[b]Electrical Engineering Dept., King Mongkut's Institute of Technology Ladkrabang, THAILAND
[c]National Science and Technology Development Agency (NSTDA), 12120 THAILAND

Abstract: - This paper focuses on a new controller design for both AC output voltage and DC voltage sides of a 3-level voltage source converter (VSC) of STATCOM based on complex transfer function. With this approach, the current regulator control with two-input two-output for the AC side of VSC can be represented by a complex transfer function with single-input single-output. In addition, the complex pole-zero compensation by the complex proportional integral (PI) controller is proposed to eliminate the cross coupling effect between the real and reactive currents in the current regulator. As a result, the practical current regulator control loop can be implemented to control the AC output voltage of VSC. For the DC side, the DC voltage control loop is also established by a PI controller. Parameters of PI controllers in both AC and DC control loops are designed by modulus optimum and symmetrical optimum criteria. Simulation results by PSCAD/EMTDC show that the proposed controller provides superior stabilizing effects on the cross coupling over the decoupling control.

Key-Words: - STATCOM, complex transfer function, voltage source converter, decoupling control

1 Introduction

The STATCOM with 3-level VSC allows both AC output voltage and DC voltage of the converter to be separately control. In general, the DC voltage is regulated at a specific value while the reactive power which depends on the AC output voltage of the converter, can be controlled by the reactive power command [1]. To achieve fast dynamic performance, the STATCOM is generally modeled in the synchronously rotating reference (dq-frame). However, its dynamic performance is slow due to the cross coupling between real and reactive current. Especially, in case of high power applications, switching devices of the converter are normally switched once a cycle to limit switching losses. Because of this low switching frequency, the cross coupling effect may cause high overshoot of the current response. To mitigate the cross coupling, many control techniques such as decoupling control and internal predictive control, have been reported in [2]-[5]. Nevertheless, their control structures are not easy to realize while control parameters tuning rules are complex. This paper proposes the new controller design methods for both current regulator control loop of AC voltage output and DC voltage control loop controller of the 3-level VSC by complex transfer function. A 3-level STATCOM connected to a typical 115 kV network is selected as a case study. Simulation studies by PSCAD/EMTDC are carried out to evaluate the control effects of STATCOM.

2 STATCOM Modeling

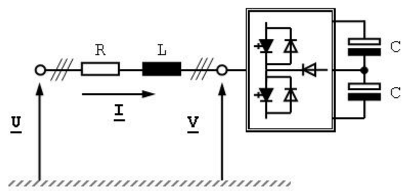

(a) equivalent circuit of the STATCOM

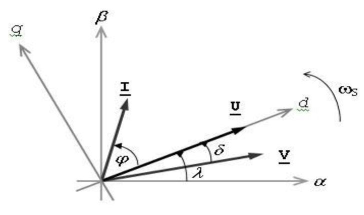

(b) complex vector diagram

Fig. 1 Complex vector model of the STATCOM

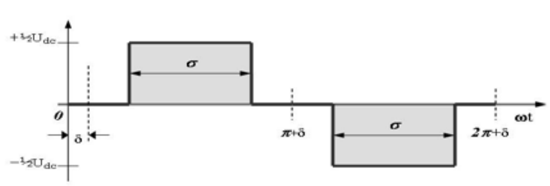

Fig. 2 Output voltage of the 3-level VSC

The circuit of STATCOM with 3-level VSC and their associated complex vectors are depicted in Fig. 1 (a) and (b), respectively. For the AC side, $\underline{U}$ is the system voltage while $\underline{V}$ is the output voltage of VSC which consists of three levels, i.e. $+\frac{1}{2}U_{dc}$, 0, and $-\frac{1}{2}U_{dc}$, as shown in Fig. 2.

The voltage equation based on complex vectors on the stationary reference frame ($\alpha\beta$-axis) of the AC system can be expressed as

$$L\frac{d\underline{I}}{dt}+R\underline{I}=\underline{U}-\underline{V} \quad (1)$$

Transforming into the synchronously rotating reference frame (dq-axis) by multiplying all terms of (1) with a unit complex vector $e^{-j\lambda}$ results in

$$L\frac{d\underline{I}_{dq}}{dt}+j\omega_S L\underline{I}_{dq}+R\underline{I}_{dq}=\underline{U}_{dq}-\underline{V}_{dq} \quad (2)$$

where ω_S is the angular speed of electrical system.

Define U_N as the base voltage, I_N as the base current, and Z_N as the base impedance, which is U_N/I_N. The normalized equation of the AC system is

$$T_1\frac{d\underline{i}_{dq}}{dt}+\left(1+j\omega_S T_1\right)\underline{i}_{dq}=\frac{1}{r}\left(\underline{u}_{dq}-\underline{v}_{dq}\right) \quad (3)$$

where $T_1=L/R$ and $r=R/Z_N$

The voltage equation (3) can be individually rewritten on d-axis and q-axis as

$$T_1\frac{di_d}{dt}+i_d-\omega_S T_1 i_q=\frac{1}{r}\left(u_d-v_d\right) \quad (4)$$

$$T_1\frac{di_q}{dt}+i_q+\omega_S T_1 i_d=\frac{1}{r}\left(u_q-v_q\right) \quad (5)$$

Note that the STATCOM model based on (4) and (5) is a two-input (v_d and v_q) two-output (i_d and i_q) system with cross coupling between real current i_d and reactive current i_q. The degree of cross coupling depends on the time constant T_1 and ω_S. To eliminate the cross coupling, the voltage equation (3) is transformed into the s domain which can be expressed by complex transfer function as

$$\frac{\underline{i}_{dq}(s)}{\underline{u}_{dq}(s)-\underline{v}_{dq}(s)}=\frac{1/r}{\left(1+j\omega_S T_1\right)+T_1 s} \quad (6)$$

Note that, (6) is a complex transfer function with single-input ($\underline{u}_{dq}(s)-\underline{v}_{dq}(s)$) and single output ($\underline{i}_{dq}(s)$).

For the VSC transfer function, it can be represented by the first-order delayed system as

$$\frac{\underline{v}_{dq}(s)}{\underline{v}^*(s)}=\frac{u_{dc}}{1+T_2 s} \quad (7)$$

where u_{dc} is a gain and T_2 is the delay time of the converter.

With V_{1N} as the base value of the magnitude of the fundamental voltage and U_{dcN} as the base DC capacitor voltage, the normalized output of the fundamental voltage waveform of the VSC in Fig.2 can be expressed as

$$|v|=\frac{|V|}{V_{1N}}=u_{dc}\sin\frac{\sigma}{2} \quad (8)$$

where $|v|$ is the normalized value of the fundamental output voltage of the VSC, u_{dc} is the normalized value of the DC capacitor voltage u_d. σ is the pulse width of the positive and negative output voltage.

The magnitude and phase angle of the complex vector $\underline{v}_{dq}$ can be controlled by the pulse width duration σ and the delayed angle δ. The control system is designed on the dq-frame. The command signal v^* is referred to the rectangular coordinates v_d^* and v_q^*. Accordingly, σ and δ can calculated by

$$\sigma=2\sin^{-1}\left(\sqrt{v_d^{*2}+v_q^{*2}}\,/u_{dc}\right) \quad (9)$$

$$\delta=\tan^{-1}\left(v_q^*/v_d^*\right) \quad (10)$$

The voltage u_d lies on the d-axis and is constant while the voltage u_q equals to zero. Thus normalized real and reactive power can be written as

$$p=u_{dc}i_{dc}=u_d i_d \quad (11)$$

$$q=-u_d i_q \quad (12)$$

For the DC side of VSC, the rate of change of capacitor voltage is related to its charging current as

$$\frac{dU_{dc}}{dt}=\frac{1}{C}I_{dc} \quad (13)$$

The based value of the real power P_N of STATCOM can be described as

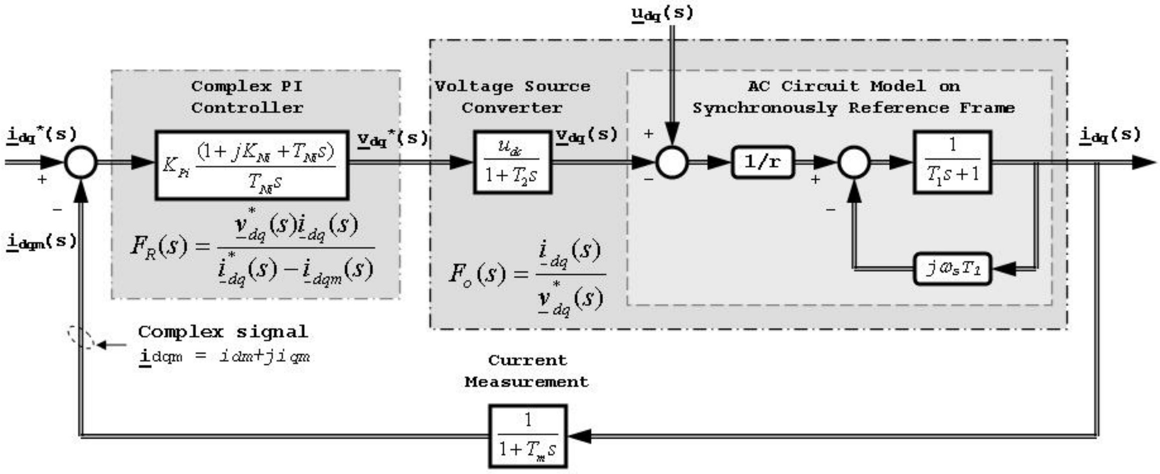

Fig. 3 Current regulator loop with complex transfer function

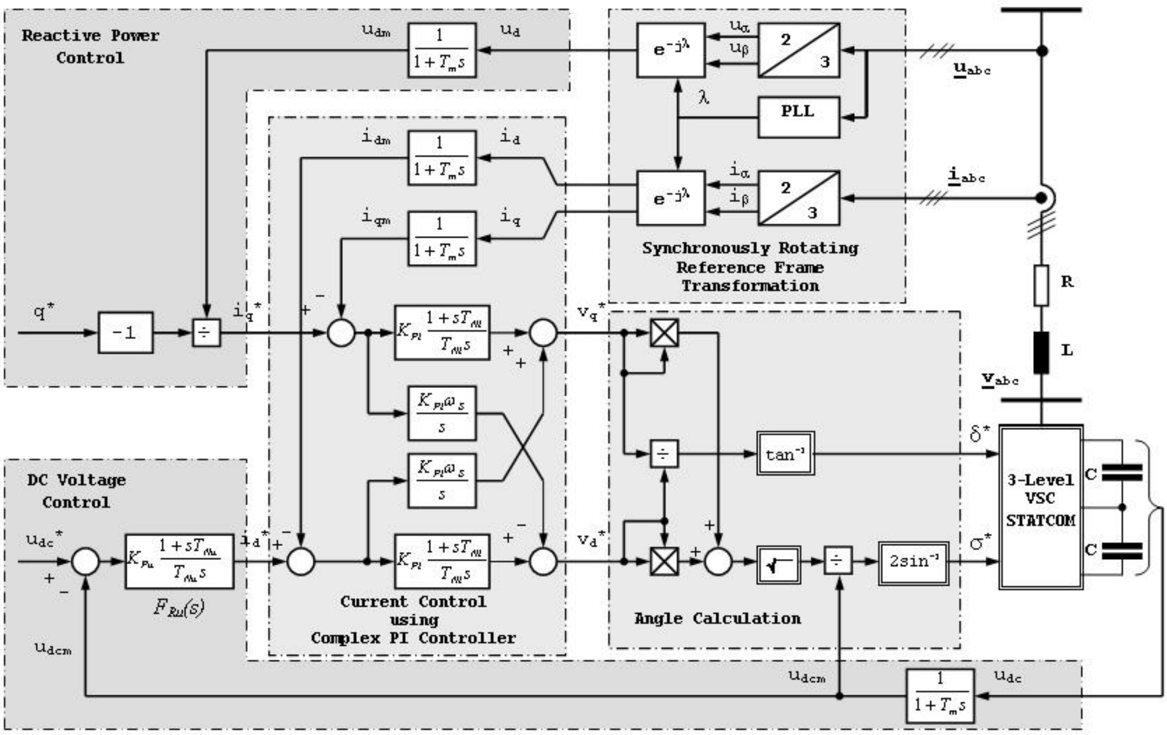

Fig. 4 Complete block diagram of the STATCOM

$$P_N = \frac{3}{2}\mathrm{Re}\left\{\underline{U}_N \underline{I}_N^*\right\} = \frac{3}{2}U_{dN}I_{dN} = U_{dcN}I_{dcN} \qquad (14)$$

where U_{dN} is the base value of the source voltage, I_{dN} is the base value of the line current on the direct axis, I_{dcN} is the base value of the DC capacitor current I_{dc}.

Therefore, the normalized DC capacitor voltage can be expressed by

$$\frac{du_{dc}}{dt} = \frac{1}{C}\frac{I_{dcN}}{U_{dcN}}\frac{u_d}{u_{dc}}i_d \qquad (15)$$

Note that (15) is a nonlinear differential equation. Linearization can be made by the assumption that the DC capacitor voltage is regulated at the set point. So u_{dc} on the right hand side of (15) is nearly constant and its derivative is very small (but not equal to zero). Hence, the transfer function of the DC capacitor voltage can be rewritten as

$$\frac{u_{dc}(s)}{i_d(s)} = \frac{1}{T_o s} \qquad (16)$$

where $T_o = C\frac{U_{dcN}}{I_{dcN}}\frac{u_{dc}}{u_d}$

3 Current Regulator Control Loop

Fig. 3 shows the block diagram of the current regulator control loop which is constructed form the AC circuit model on the synchronously rotating reference frame in (6) and a voltage source converter transfer function in (7). As shown in Fig.3, the open loop transfer function can be expressed by

$$F_o(s) = \frac{\underline{i}_{dq}(s)}{\underline{v}^*_{dq}(s)} = \frac{1/r}{(1 + j\omega_S T_1) + T_1 s}\frac{u_{dc}}{1 + sT_2} \qquad (17)$$

The open loop poles of (17) consists of a single complex pole from AC circuit model $(-1/T_1 - j\omega_S)$ which is located in the third quadrant of the complex plane, and a real pole of the voltage source converter $(-1/T_2)$ which is located in the left half plane. The complex pole $(-1/T_1 - j\omega_S)$ causes the cross coupling effect. This effect is an inevitable problem in the ac side which causes sluggish response and high overshoot of the current. To overcome this problem, the complex pole-zero compensation technique [6, 7] is applied.

As observed in Fig.3, the complex PI controller $F_R(s)$ is connected in series with $F_o(s)$ in order to compensate the cross coupling pole $(-1/T_1 - j\omega_S)$. Therefore, the open loop transfer function of the system including the complex PI controller is

$$F_R(s)F_o(s) = \frac{K_{Pi}(1 + jK_{Ni} + T_{Ni}s)}{T_{Ni}s}\frac{1/r}{(1 + j\omega_S T_1) + T_1 s}\frac{u_{dc}}{1 + T_2 s} \qquad (18)$$

By setting $K_{Ni} = \omega_S T_1$ and $T_{Ni} = T_1$, the new open loop transfer function becomes a second order system as

$$F_R(s)F_o(s) = \frac{K_{Pi}}{T_{Ni}s}\frac{1}{r}\frac{u_{dc}}{1 + T_2 s} \qquad (19)$$

The controller gain K_{Pi} is adjusted to achieve fast dynamic response to the current command with small overshoot. Thus, the damping factor of the closed loop system is set at 0.707. Accordingly, the modulus optimum (MO) criterion can be applied to set the controller gain as

$$K_{Pi} = \frac{1}{2}\frac{r}{u_{dc}}\frac{T_1}{T_e} \qquad (20)$$

where T_e is the summation of the converter time delay T_2 and time delay of the current measurement T_m. Note that the input signal of the complex PI controller is the difference between the command current i^*_{dq} and the measured current i_{dq}. In addition, the PI controller is based on a complex transfer function with complex signal input and output. It can not be implemented in practice.

To realize the complex PI controller in Fig.3, the transfer function $F_R(s)$ is expressed on d-axis and q-axis as in (21)-(23).

$$\begin{aligned} F_R(s) &= \frac{\underline{y}_R(s)}{\underline{x}_R(s)} = \frac{y_d(s) + jy_q(s)}{x_d(s) + jx_q(s)} \\ &= K_{Pi}\frac{(1 + j\omega_S T_{Ni} + T_{Ni}s)}{T_{Ni}s} \end{aligned} \qquad (21)$$

$$\begin{aligned} y_d(s) &= \frac{K_{Pi}}{T_{Ni}s}\left\{x_d(s) + T_{Ni}sx_d(s) - \omega_S T_{Ni}x_q(s)\right\} \\ &= K_{Pi}\frac{(1 + T_{Ni}s)}{T_{Ni}s}x_d - \frac{K_{Pi}\omega_S}{s}x_q \end{aligned} \qquad (22)$$

$$\begin{aligned} y_q(s) &= \frac{K_{Pi}}{T_{Ni}s}\left\{x_q(s) + T_{Ni}sx_q(s) + \omega_S T_{Ni}x_d(s)\right\} \\ &= K_{Pi}\frac{(1 + T_{Ni}s)}{T_{Ni}s}x_q + \frac{K_{Pi}\omega_S}{s}x_d \end{aligned} \qquad (23)$$

where $\underline{y}_R$ is the complex signal of the output of the controller, $\underline{x}_R$ is the complex signal of the input of the controller, y_d is the input signal on d-axis, x_d is the input signal on d-axis, y_q is the input signal on q-axis, x_q is the input signal on q-axis.

Based on (22) and (23), the complex PI controller can be constructed by two PI controllers and two I controllers. Thus, the block diagram of the current regulator in Fig. 3 can be realized in Fig.4. The outputs of the complex PI controller are *d*-axis and *q*-axis voltage commands v_d* and v_q*. These signals are used to calculate the pulse duration σ and delayed angle δ signals of VSC by (9) and (10), respectively, as depicted in Fig. 4.

To simplify the system modeling, the current regulator in Fig. 4, can be approximated as

$$\frac{i_d(s)}{i^*_d(s)} = \frac{1}{1 + 2T_e s + 2T_e^2 s^2} \approx \frac{1}{1 + 2T_e s} \qquad (24)$$

$$\frac{i_q(s)}{i_q^*(s)} = \frac{1}{1+2T_e s+2T_e^2 s^2} \approx \frac{1}{1+2T_e s} \tag{25}$$

This approximated transfer functions will be used in the design of DC voltage control loop.

4 DC Voltage Control Loop and Reactive Power Control

Assuming that the current regulator is perfectly decoupled and the source voltage is constant, the reactive power can be directly controlled by the reactive current i_q. The reactive current command i_q* is determined by reactive power command q* and the measured voltage on d-axis as

$$i_q^* = -\frac{q^*}{u_{dm}} \tag{26}$$

As a result, the reactive power controller block can be shown in Fig. 4.

Next, the model of the DC capacitor voltage (16) is integrated into to system in Fig. 4. The DC voltage is controlled by the real current i_d. The purpose of this control loop is to regulate the DC voltage at a desired value. Hence, the disturbance rejection is the main objective of the controller design. The open loop transfer function in the DC voltage control loop in Fig. 4 is a cascaded transfer function of the DC voltage transfer function (16), the approximation of the current regulator (24) and the PI controller ($F_{Ru}(s)$) which can be represented as

$$F_{Ru}(s).\frac{i_d(s)}{i_d^*(s)}.\frac{u_{dc}(s)}{i_d(s)} = \frac{K_{Pu}(1+T_{Nu}s)}{T_{Nu}s}.\frac{1}{1+2T_e s}.\frac{1}{T_o s} \tag{27}$$

According to symmetrical Optimum (SO) criteria [8], [11], the controller integral time constant T_{Nu} and the controller gain K_{Pu} can be calculated by

$$T_{Nu} = 4(2T_e + T_m) \tag{28}$$

$$K_{Pu} = \frac{1}{2}\frac{T_o}{(2T_e + T_m)} \tag{29}$$

By integrating both current regulator control loop and DC voltage control into the converter control, the complete block diagram of the proposed controller can be shown in Fig. 4.

5 Simulation Results

A 12-pulse STATCOM employing 3-level VSC circuit is shown in Fig. 5. The rating of the STATCOM is 100 Mvar. It is connected to a 115 kV 50 Hz AC power system. Simulation studies are carried out by PSCAD/EMTDC. System parameters are given in an Appendix.

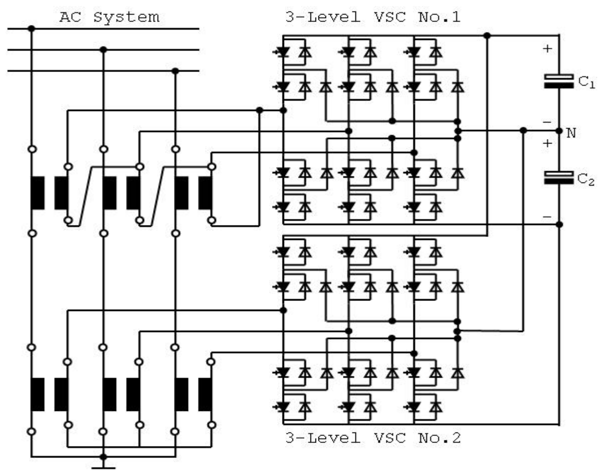

Fig.5. a 12-pulse STATCOM with 3-level VSC

The STATCOM produces reactive power q according to reactive power command q* while the DC voltage U_{dc} is regulated at 1.15 per-unit. Fig. 6 shows dynamic responses of the measured real i_{dm} and reactive current i_{qm} of the proposed control in comparison with those of the decoupling control method. The step command of the reactive power q is changed from -0.75 per-unit (generate) to +0.75 per-unit (absorb). According to (24), this also causes the change in reactive current command i_q* from +0.75 per-unit to -0.75 per-unit. It can be seen that the reactive currents of both methods respond with short rise time (less than 20 ms) and small overshoot. Nevertheless, the proposed control reaches steady state faster.

The changes in the real current (i_{dm}) was very small for this proposed method and it reached steady state in a very short time. On the contrary, real current idm of the decoupling control method fluctuated in a wide range as much as 300%.

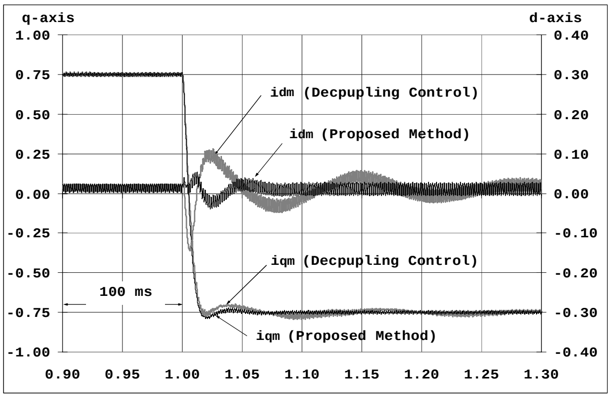

Fig.6. Step response of the real and reactive current

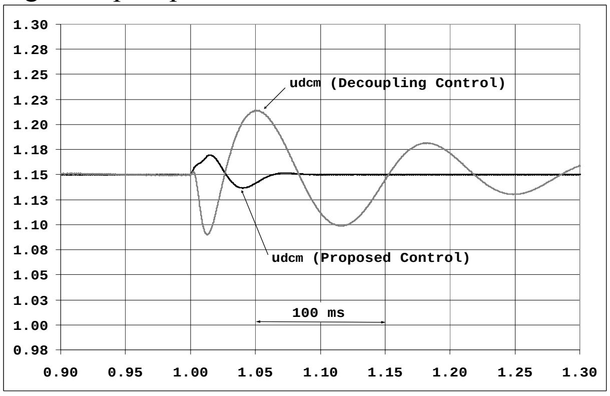

Fig.7. Step response of the DC voltage

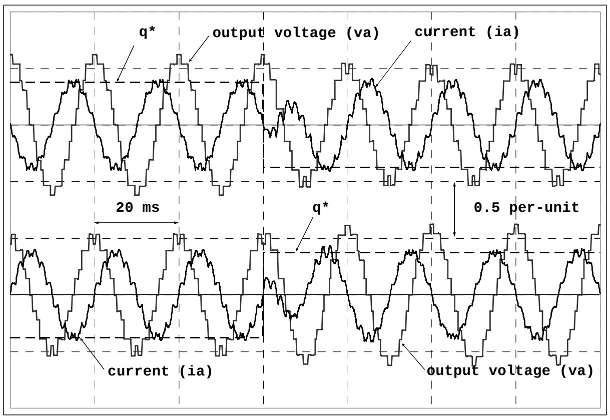

Fig.8. Voltage and current waveforms

Fig. 7 shows the dynamic responses of the measured DC voltage u_{dcm} against the step command in comparison to the decoupling control method. The proposed controller is able to damp the oscillation significantly. On the contrary, in case of decoupling control, the DC voltage severely oscillates due to the cross coupling effect. It takes long time to reach steady state. Because the time delays of converter and measurement system are generally neglected in the decoupling control. The cross coupling effects can not be eliminated. It should be noted that for the converter employing line frequency switching, the delay times must be taken in to consideration in the decoupling control.

Fig.8 depicts the voltage and current output waveforms of STATCOM with the proposed control during step reactive power commands in case of from leading to lagging (above) and lagging to leading (below). It can be seen that the phase of the current waveform can be reversed within a half cycle in both cases.

6. Conclusion

The controller design for AC and DC voltage control loops based on complex transfer function for a 3-level VSC of STATCOM has been presented. The current regulator with two-input two-output is represented by a complex transfer function with single-input single-output. The cross coupling in the current regulator for AC side is eliminated by the complex pole-zero compensation based on the complex PI controller. The control parameters of PI controllers of both AC and DC voltage sides can be systematically designed. This makes the proposed controller very practical and easy to realize in actual power systems. Simulation results confirm that the proposed controller is capable of reducing the cross coupling effectively in comparison to the decoupled control.

In the future work, more simulation studies under disturbances will be carried out. Besides, the proposed control design will be applied to UPFC.

Appendix

Transformer %Z = 10%, Cu-losses = 2%, No.1 50 MVA 33.2/16.0 kV, No.2 50 MVA 33.2/9.24 kV
Capacitor C1 and C2 = 6400 μF, T_{Ni} = 15.92 ms and K_{Pi} = 0.055, T_{Nu} = 26.72 ms and K_{Pu} = 1.16

References:

[1] N. G. Hingorani, and L. Gyugyi, *Understanding FACTS*, IEEE Press, 2001.

[2] Guk C. Cho, et al, "Analysis and Controller Design of Static Var Compensator Using Three-Level GTO Inverter", *IEEE Trans. Power Electronics*, Vol. 11, 1996, pp. 57-65.

[3] I. Papič, et al, "Basic Control of Unified Power Flow Controller", *IEEE Trans. Power Systems*, Vol. 12, 1997, pp. 1734-1739.

[4] P. García-González and A. García-Cerrada, "Detailed Analysis and Experimental Results of the Control System of a UPFC", *IEE Proc. Part C*, Vol. 150, 2003, pp. 147-154.

[5] S. D. Round, et al, "Performance of a Unified Power Flow Controller using a D-Q Control

System", *Proc. 6th IEE Conf. on AC and DC Power Transmission*, 1996, pp. 357-362

[6] F. Briz, et al, "Analysis and design of current regulators using complex vectors ", *IEEE Trans. Ind.App.*, Vol.36, 2000, pp. 817-825

[7] J. Holtz, et al, "Design of Fast and Robust Current Regulators for High-Power Drives Based on Complex State Variables", *IEEE Trans. Ind. App*, Vol. 40, 2004, pp. 1388-1397.

[8] S. Gataric, "Modelling and Design of Three-Phase System Using Complex Transfer Function", *Proc. 30th IEEE Conf. on Power Electronics Specialists*, 1999, pp. 691-697.